



**HAL**  
open science

## Advanced design of a X-ray Absorption Spectroscopy setup for measuring transition metals speciation in molten carbonates, hydroxides and hydrogensulfates

Z. Safarzadeh, J. Gomes, J. Sirieix-Plénet, N. Ruiz, L. Hamitouche, L. Michot, L. Carré, L. Barthe, V. Briois, A.-L. Rollet

### ► To cite this version:

Z. Safarzadeh, J. Gomes, J. Sirieix-Plénet, N. Ruiz, L. Hamitouche, et al.. Advanced design of a X-ray Absorption Spectroscopy setup for measuring transition metals speciation in molten carbonates, hydroxides and hydrogensulfates. *Review of Scientific Instruments*, 2022, 93 (7), pp.075102. 10.1063/5.0087698 . hal-03774823

**HAL Id: hal-03774823**

**<https://cnrs.hal.science/hal-03774823>**

Submitted on 12 Sep 2022

**HAL** is a multi-disciplinary open access archive for the deposit and dissemination of scientific research documents, whether they are published or not. The documents may come from teaching and research institutions in France or abroad, or from public or private research centers.

L'archive ouverte pluridisciplinaire **HAL**, est destinée au dépôt et à la diffusion de documents scientifiques de niveau recherche, publiés ou non, émanant des établissements d'enseignement et de recherche français ou étrangers, des laboratoires publics ou privés.

# Advanced design of a X-ray Absorption Spectroscopy setup for measuring transition metals speciation in molten carbonates, hydroxides and hydrogenosulfates

Z. Safarzadeh,<sup>1,2, a)</sup> J. C. Gomes,<sup>1</sup> J. Sirieix-Plénet,<sup>1,2</sup> N. Ruiz,<sup>1,2</sup> L. Hamitouche,<sup>1,2</sup> L. Michot,<sup>1</sup> L. Carré,<sup>3</sup> L. Barthe,<sup>4</sup> V. Briois,<sup>4</sup> and A.-L. Rollet<sup>1,2</sup>

<sup>1)</sup>Sorbonne Université, CNRS, laboratoire PHysico-chimie des Électrolytes et Nanosystèmes Interfaciaux (PHENIX), F-75005 Paris, France

<sup>2)</sup>Réseau sur le Stockage Electrochimique de l'Energie (RS2E), FR CNRS 3459, F-80000 Amiens, France

<sup>3)</sup>PSL Research University, Chimie Paristech, CNRS, Institut de Recherche de Chimie de Paris (IRCP), F-75005 Paris, France

<sup>4)</sup>Synchrotron SOLEIL, F-91192, Gif-sur-Yvette, France

(\*Authors to whom correspondence should be addressed: valerie.briois@synchrotron-soleil.fr and anne-laure.rollet@sorbonne-universite.fr)

(Dated: 12 September 2022)

Battery recycling is currently becoming a crucial issue. One possible treatment path involves the use of molten salts. Mechanistic understanding of the underlying processes requires being able to analyze in-situ speciation in the molten salts at various temperatures. This can be advantageously achieved using X-ray absorption spectroscopy, the use of Quick-EXAFS facilities being particularly appropriate. Consequently, this paper presents the design and development of a new setup allowing to carry out Quick-EXAFS experiments in molten oxidizing salts at high temperature. We describe the different components of the cell and the performances of the heating device. We illustrate the capabilities of the set-up by analyzing the temperature evolution of Co speciation upon dissolution of LiCoO<sub>2</sub>, a typical battery electrode material, in molten carbonates, hydroxides and hydrogenosulfates.

## I. INTRODUCTION

Recycling is becoming a crucial issue for Human societies to reduce environmental hazards while recovering essential resources that are becoming scarcer<sup>1,2</sup>. This is particularly acute when considering the explosion of mobile technologies that generates tremendous amounts of Lithium battery wastes<sup>3</sup>. Currently, various drawbacks prevent an efficient recycling of these materials<sup>4</sup>. First, lithium batteries are using a wide range of technological solutions<sup>5,6</sup> implying various electrode materials, different electrolytes, etc. Second, there is a significant time lag between their end of life and their arrival in the recycling circuit, due to their conservation by consumers even long after their end of use. Third, they are composed with parts belonging to various chemical families, i.e. metals, oxide and organic matter that require the use of very distinct recycling methods.

Most publications dealing with lithium battery recycling focus on the electrode materials and employ hydrometallurgical processes<sup>7–10</sup>. In contrast, only few papers report on the use of pyrochemical processes<sup>11–13</sup>, i.e. chemistry in molten salts, whereas such techniques present definite appealing aspects. Pyrochemistry, that is used in metallurgy for decades<sup>14–16</sup>, has indeed already been applied for various waste treatment operations as illustrated by the following examples. The use of molten fluorides and molten chlorides has been proposed for nuclear waste treatment<sup>17–19</sup>. Molten carbonates have

proven very efficient for organic compounds degradation and have been used to treat long polymer chains, i.e. plastics<sup>20–22</sup> as well as volatile and hazardous molecules, like CCl<sub>4</sub> and C<sub>6</sub>H<sub>5</sub>Cl<sup>23–25</sup>. They can sometimes be mixed with hydroxides to decrease the running temperature<sup>26,27</sup>. Molten hydroxides dissolve numerous metals<sup>28</sup> and oxides<sup>29</sup>. Considering the variety of situations in which molten salts provide viable recycling solutions, they clearly represent relevant alternatives to hydrometallurgical processes for Lithium battery recycling. In particular, oxidizing molten salts, such as carbonate, sulphate, nitrate, hydroxide, phosphonate, etc. appear promising and their use deserves further evaluation.

In the present paper, we focus on the reaction of battery electrode components in molten salts and try to shed new light on the underlying mechanisms. This clearly requires being able to assess the evolution with temperature of the oxidation state and speciation of metals inside the molten salts. These features can be efficiently analyzed by X-ray Absorption Spectroscopy (XAS) and the question then arises whether XAS studies can be performed in the highly demanding conditions associated to molten salts, i.e. high temperature and corrosiveness. Several studies already addressed this issue and a few XAS studies on metal speciation in molten halides can be found in the literature<sup>30–35</sup>. Depending on the salt used, different technical solutions were proposed. Quartz can be used with chloride or bromide media but it is dissolved in the presence of fluorides. For this reason, boron nitride cells are used for fluorides but their tightness is insufficient for their use with chlorides. In the specific case of radioactive molten fluoride salts, additional shields have to be added<sup>36,37</sup>. In parallel, several works addressed the case of molten oxides<sup>38–40</sup>.

To the best of our knowledge, the case of molten oxidiz-

<sup>a)</sup>Also at Sorbonne Université, CNRS, laboratoire de la Molécule aux Nano-Objets : Réactivité, Interactions et Spectroscopies (MONARIS), F-75005 Paris, France

ing salt has not been investigated yet. In the present publication, we describe the design of a specific setup allowing to carry out high temperature X-ray absorption spectroscopy (HT XAS) experiments in molten carbonates, hydroxides and hydrogenosulphates. We will apply this set up to study the dissolution of  $\text{LiCoO}_2$ , a typical battery electrode material on the ROCK beamline of SOLEIL synchrotron that is dedicated to fast XAS measurements<sup>41</sup>.

## II. SETUP DESIGN

The analysis by XAS of the speciation of transition metals in molten oxidizing salts imposes the following conditions: running temperature up to  $650^\circ\text{C}$  with a stability of  $2^\circ\text{C}$ , atmosphere control or air-tightness, cell materials that do not leak and are inert to both molten salts and transition metals and optimized optical path to allow measurements in transmission mode. Herein for K edge threshold energies of the 3d chemical elements composing the materials electrodes, the optical path is less than half millimeter. In addition, the setup should allow the sample to rapidly reach the running conditions, i.e. thermal equilibrium, in order to evidence using Quick-EXAFS the presence of transitory compounds that could appear upon reaction of  $\text{LiCoO}_2$  with the molten salt below and above the liquidus temperature.

The present cell design is inspired by previous developments dedicated to molten halides<sup>30,32,33,42</sup>. For clarity, let us recall the main features of these cells. For measuring XAS spectra of rare earth and actinides in molten chlorides<sup>42</sup>, a flat quartz vial with a reservoir at the top had been designed. The aim of the reservoir was to ensure a complete filling of the cell at the optical path area, once the salt melts. The thickness of the optical path was fixed and determined by the distance between quartz walls. The vial could be sealed, which guarantees a perfect control of the chloride salt, i.e. no hydration by surrounding atmosphere. Nevertheless, such a design does not allow easy studies of elemental concentrations. For the measurement of XAS spectra of rare earth and actinides in molten fluorides<sup>32</sup>, the cell design was based on two high purity and high density boron nitrides plates. A hollow cavity was formed in the plates that were maintained together with screws. There was no reservoir and the control of salt filling at the optical path zone was ensured by dispersing the salt within a solid matrix composed of boron nitride powder. An advantage of this procedure is that it enables an easy study of concentration effects.

In the present case of molten oxidizing salts, two kind of cells have been designed: with and without reservoir. The target melting temperatures evolve from  $860^\circ\text{C}$  for molten carbonates ( $\text{Na}_2\text{CO}_3$ ), to  $470^\circ\text{C}$  for hydroxides ( $\text{LiOH}$ ) and  $197^\circ\text{C}$  for hydrogenosulfates ( $\text{KHSO}_4$ ). For practical recycling operations, one generally uses eutectic compositions that lower the melting temperatures. The cell design then allowed reaching temperatures up to  $650^\circ\text{C}$  but the experiments were limited to  $550^\circ\text{C}$ . At high temperature, it is crucial to control the atmosphere and, in particular, the oxygen level because (i) molten salt oxidation efficiency depends on the oxoacidity that

TABLE I. Amount of sample and Co in the X-ray beam

Molten Salt	[LiCoO <sub>2</sub> ] in molten salt (wt%)	sample mass for jump of 1 (mg/cm <sup>2</sup> )
[Li <sub>2</sub> CO <sub>3</sub> -Na <sub>2</sub> CO <sub>3</sub> -K <sub>2</sub> CO <sub>3</sub> ] <sub>eutectic</sub>	10	51.3
NaHSO <sub>4</sub>	21.4	26.0
LiOH	10	51.2

depends itself on the oxygen concentration in the atmosphere, and (ii) the cell itself may be damaged by combustion. In addition, as the K edge of classical 3d transition metals such as Mn, Co and Ni is located at relatively low X-ray energy ( $E_{Mn} = 6539$  eV,  $E_{Co} = 7709$  eV and  $E_{Ni} = 8333$  eV), and in order to minimize the absorption by the cell, its design requires the use of materials with light chemical elements, easily manufactured as thin X-ray windows encapsulating a sample within a cavity with a short optical path. As an illustration, Table 1 lists different samples that were analyzed and the amount of sample needed for obtaining an edge jump of 1.

### A. Cell

The schemes of the two cell designs are presented in Fig. 1 (additional pictures are available in the supplementary information file). Each cell is entirely composed of two boron nitride (BN) cuboids 4 cm long, 2.5 cm wide and 1cm thick. The technical schema is given in supplementary materials. This material has already been selected for HT XAS studies in molten fluorides and in that case, stringent specifications on the amount of oxide present in the material had to be applied. In the case of oxidizing molten salts, the presence of oxide in BN is much less crucial. Accordingly, HP grade boron nitride was selected, because of its higher compactness than that of oxide free boron nitride. It has been purchased from Final Advanced Materials. The thickness of each BN block, i.e. 1 cm is rather high compared to the 1 mm thickness used for molten fluorides. This choice of a higher thickness has a dual objective. First, it allows drilling a hole through the BN block to insert a thermocouple located very close ( $\approx 5\text{mm}$ ) to the area at which XAS measurement are performed, which ensures excellent temperature control. Second, it is possible to hollow a reservoir large enough to get complete salt filling at the measurement zone once the salt melts. As illustrated in Fig. 1 the reservoir is located in continuation of the cavity ( $D_1$ ). Third, it is possible to make thin wall to minimize the X-ray absorption by the cell.

In the first cell design, a cavity, 200 to 400  $\mu\text{m}$  in depth, 8 mm large and 25 mm high, is drilled in the block for receiving the salt in the measurement zone. The back side is hollowed in the region where the X-ray beam will pass to reach a BN plate thickness less than 300  $\mu\text{m}$ . The back side of the second BN block (lid) is hollowed in the same way (Fig. 1). Hence, the total BN length yielding an increase X-ray transmission is less than 600 $\mu\text{m}$ . In addition, a groove is made all along the interior part edge of the cell in order to improve gluing. The

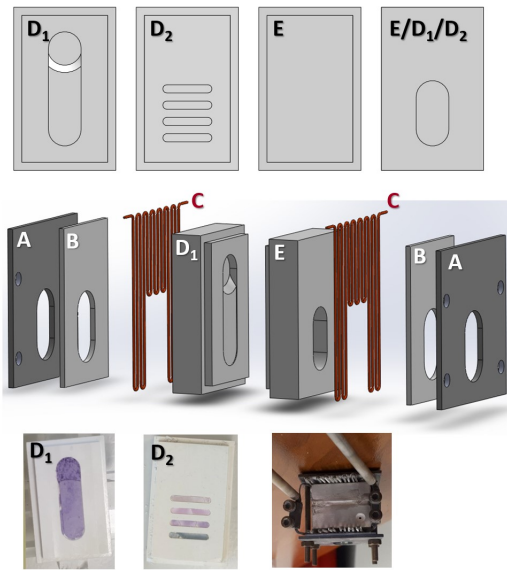


FIG. 1. At the top, schemes of the boron nitride cells: internal side of the one compartment cell ( $D_1$ ), of the four compartments cell ( $D_2$ ) and of the cell lid (E), external side of both cell parts. In the middle, schematic exploded view of the cell and heating device: the inox plate (A), the boron nitride plate (B), the kantal heating wire (C), the one compartment cell ( $D_1$ ) and its lid (E). At the bottom, pictures of the one compartment ( $D_1$ ) and four compartments ( $D_2$ ) cells filled with samples and top view of the cell sandwiched with the heating device.

two parts of the cells are closed together either by gluing the borders using an alumina ceramic glue (Resbond® 989F purchased from Final Advanced Materials) or by using screws. It is important to note that the interior surface of both parts has been carefully flattened to ensure optimal contact between plates and hence to prevent salt leakage at high temperature. The quality of the surface is illustrated by (i) the sucking effect when  $D_1$  is leaned over E, (ii) the fact that the gas is retained inside the chamber during experiments (see discussion). The quality of the surface also prevents the ceramics glue from diffusing inside the cell cavity. After experiments, no sign of glue has been observed on the inert parts of the cell.

The second cell design does not bear any reservoir, but contains four cavities (Fig. 1). The rationale of such a design is linked to the fact that in HT XAS experiments, the time limiting factor is not associated to spectra recording but to temperature ramps and stages. Hence, the use of several cavities within one cell, allows recording up to 4 samples in one run. Each cavity is 2 mm high and 8 mm large. In this second cell design, the salt is dispersed within a BN powder matrix. The aim is there to maintain an homogeneous salt distribution inside the cavity.

In both cells, the salt is introduced as pellets (pressed at 14 tons) to facilitate and optimize cavity filling.

Finally, the same cell made in graphite has been tested and it yields to similar results for carbonate and hydrogensulfate molten salts.

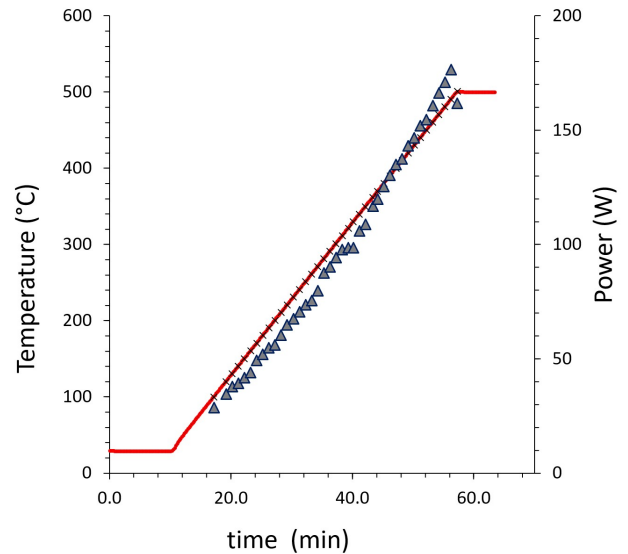


FIG. 2. Sample temperature (red dot), temperature set point (black cross) and power (triangle) as a function of the time.

## B. Heating device

The scheme and picture of the heating device are shown in Fig. 1. It consists in two wires of kantal (add the resistance of the wire) 500 mm long, weaved along each large face of the cell. They are connected to each other and to the electrical cables on the lateral side thanks to two electrical lusters. The cell and wires are sandwiched between two hollowed stainless steel plates maintained by four screws that ensure that all parts stay in the right position and optimize the contact of the wire with the boron nitride cell. Two thin hollowed BN plates are placed between the wires and the stainless steel plates to prevent electrical contact. The electrical cables (500 mm) consist in copper twisted wires. They should be replaced after approximately 100 hours of running.

The heating elements have been connected to an electrical power supply (Delta Elektronika SM52-30 (52V, 30A, 1500W)). The temperature is controlled thanks to a home made Rock design device that combines a Eurotherm 2408 controller, a Eurotherm 2408-i display, both integrated within a security and command system. To illustrate the quality of the heating, the temperature and the delivered power are plotted versus time in Fig. 2. The data are taken during the temperature ramp (10°C/minute) up to 500°C. The temperature control system (closed-loop PID control) behaves efficiently. The increase in power to monitor the setpoint temperature is very stable, with no notable variations. This power stability induces a fine control of the sample temperature. In addition, it can be noted that the rise in temperature of the sample is indeed linear, and constant with respect to the set temperature. The quality of the behavior of these 2 parameters, power and temperature, demonstrates an efficient oven design, both in terms of the heating element and the thermal insulation.

This setup allows to reach 650°C with a stability of +/- 1°C

with a temperature ramp up to 20°C/min.

### C. Chamber

Cell and heating elements are placed inside a chamber for the measurements. This chamber has several objectives. First, it allows controlling the atmosphere around the cell and heating device. At high temperature, graphite and boron nitride can burn in the presence of oxygen. Accordingly, it is crucial that all the sensitive pieces are placed in an inert atmosphere during the high temperature experiment. In the present study, we used N<sub>2</sub> gas flow. For this purpose, the gas inlet and outlet were placed on the lateral and upper parts, respectively. Second, the chamber maintains the cell and heating device in the appropriate position with respect to the X-ray beam and allows a quick installation in the beamline. The design of the chamber and a picture of the whole set-up positioned on the beamline are presented in Fig. 3. The chamber itself is placed on top of an aluminum platform that is adapted for fast mounting on the ROCK beamline. The chamber is composed of 5 aluminum plates screwed to each other and to the motorized sample stage of the platform. The front and back plates are hollowed and covered by a Kapton film for the beam path letting the X-ray beam transmission and making air-tight the chamber. On the upper plate, three additional holes are made for introducing the thermocouple (type K) and the electric cables for the heating elements. To minimize the heat transfer to the aluminum parts, the cell and heating elements are enclosed in a ceramic chamber Fig. 3. The latter is made in alumina silicate cement (Rescore® 750) purchased from Final Materials and consist of a base, a surrounding wall with holes for the beam path and an upper part with three holes for introducing the thermocouple and the electric cables. To ease the mounting, the upper part is cut in two pieces. In addition, the thermocouple and the electric cables are introduced in rigid alumina tubes to rigidify them and ease their placement. Outside the chamber, the electric cables are placed in alumina ceramic fibers for electrical insulation. Finally, the electric cables are connected thanks to a ceramic luster to the electrical power supply (Delta Elektronika SM5230 1500W). This connection prevents any undesirable motions of the cell and heating elements during the last stages of installation on the beamline.

## III. EXPERIMENT

### A. Samples

Li<sub>2</sub>CO<sub>3</sub>, K<sub>2</sub>CO<sub>3</sub> were purchased from Prolabo (AnalaR normapur grade) and Na<sub>2</sub>CO<sub>3</sub> from Sigma Aldrich (purity ≥ 99.0%). LiOH was purchased from Prolabo (AnalaR normapur grade). NaHSO<sub>4</sub> was purchased from Sigma Aldrich (purity ≥ 99%). Cathode materials LiCoO<sub>2</sub> were purchased from Sigma Aldrich (purity ≥ 99.8%). The salts were dried in a stove and stocked in a glove box under Ar before being mixed with LiCoO<sub>2</sub>. In the present case, the cells have

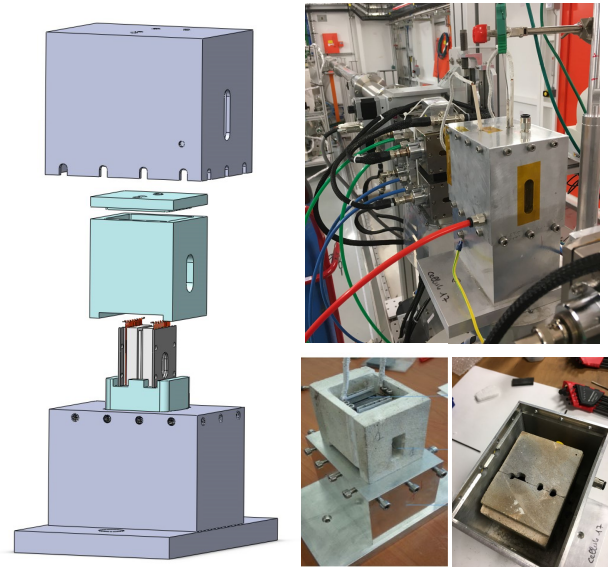


FIG. 3. On the left, exploded view of the aluminium and ceramic chambers and the cell sandwiched with the heating device. On the right, pictures of the chamber installed on ROCK beamline (top), the ceramic chamber placed on the base of the aluminium chamber (bottom left) and the ceramic chamber with its lid placed inside the aluminium chamber (bottom right).

been filled outside the glove-box under ambient atmosphere, i.e. the salts were pressed as pellets outside the glovebox and these pellets were introduced in the cell under open atmosphere.

### B. XAS measurement

X-ray absorption spectroscopy experiments were performed at the Cobalt K edge (7709 eV) at the ROCK Quick-EXAFS beamline of the synchrotron SOLEIL (France). XAS spectra were acquired in transmission mode with three ionization chambers: one before the sample, a second one located after the sample for measuring sample transmission and a third one located after a Co metallic foil used as an internal reference for energy calibration. The energy was calibrated at 7709 eV at the maximum of the first derivative measured for the Co metallic foil. The measurement was performed over the range 7510-8300 eV using a 1.5° oscillation amplitude of the Si(111) channel-cut Quick-EXAFS monochromator at a frequency of 2 Hz allowing to measure one spectrum every 250 ms. Taking advantage of the small beam size available at the focusing positions of the beamline optics (FWHM 370 μm x 300 μm horizontal x vertical), 10 mm wide line scans of the cell with step of 250 μm at 37 different vertical positions along the cell (each position being separated by 500 μm) has been performed with integration time for photon counting of 0.1 s per position. The repetition of such scanning at two different energies taken before (7550-7650 eV) and after (7770-7830 eV) the Co K edge energy allows us to localize cobalt within

the cell cavity using Matlab® script for rebuilding absorption contrast maps. Massive normalization of the Quick-EXAFS data were performed using the normal\_gui python Graphical User Interface available at the ROCK beamline<sup>43</sup>.

#### IV. RESULTS

LiCoO<sub>2</sub> and NaHSO<sub>4</sub> were mixed with 50% wt of BN to adjust the sample transmission and achieve an edge jump close to 1. The inertness of BN with LiCoO<sub>2</sub> and NaHSO<sub>4</sub> upon heating treatment was confirmed by ex situ XRD analysis. The mixed powders were pressed into pellets and placed in the cell. The heating rate was 3.5°/min from room temperature to 650°C.

To illustrate the efficiency of our setup, we present the case of LiCoO<sub>2</sub>, a widely used electrode material in Lithium batteries, in three molten salts: [Li<sub>2</sub>CO<sub>3</sub>-Na<sub>2</sub>CO<sub>3</sub>-K<sub>2</sub>CO<sub>3</sub>]<sub>eutectic</sub>, LiOH and NaHSO<sub>4</sub>.

##### A. Carbonates

We use the eutectic composition of Li<sub>2</sub>CO<sub>3</sub>-Na<sub>2</sub>CO<sub>3</sub>-K<sub>2</sub>CO<sub>3</sub> that corresponds to the mixture of 43.5mol% of Li<sub>2</sub>CO<sub>3</sub>, 31.5mol% of Na<sub>2</sub>CO<sub>3</sub> and 25mol% of K<sub>2</sub>CO<sub>3</sub>. Its melting temperature is 405°C. The salt was dried at 100°C for several days in order to avoid moisture. Significant spectral changes are observed with increasing temperature like white line intensity changes and slight energy shift of the rising edge (see the figure inset in Fig. 4) and resonances beyond the edge. Indeed, melting can generally be evidenced from a modification of the XAS oscillation that damp<sup>44</sup>. In the present case, no significant damping of the XAS oscillations is observed (Fig. 4). This may be due either to the fact that cobalt remains "stuck" in nanoparticles or to an incomplete filling of the cell upon melting. To discard this latter possibility we mapped the cell before and after heating at two different energies, below and above the Co K edge (Fig. 5). The change in the difference maps before and after heating clearly evidences that melting had occurred during the experiment. It then appears likely that in such a system cobalt nanoparticles preexist and do not seem to be affected upon melting.

##### B. Hydrogenosulfates

The melting temperature of NaHSO<sub>4</sub> is 186°C. In contrast with the previous case, the mixture was not heated before the HT XAS experiment. Pristine LiCoO<sub>2</sub> was then mixed with NaHSO<sub>4</sub> in a one to four ratio before being introduced in the HT cell. The temperature evolution of the Co transmission spectra as a function of temperature is displayed in Fig. 6. In that case, major spectral changes can be observed with increasing temperature. At a temperature value close to 186°C, oscillations start dampening while a shift in position of the edge towards lower energy can be observed. Such dampening indicates the onset of melting. A continuous change of

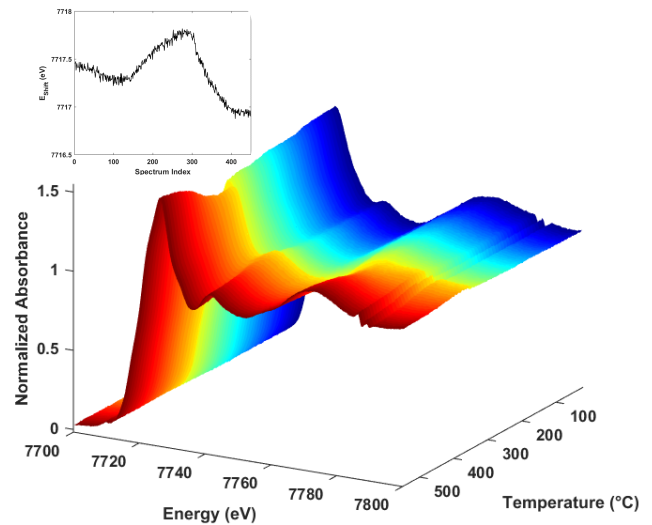


FIG. 4. Co K edge spectra in the case of LiCoO<sub>2</sub> in [Li<sub>2</sub>CO<sub>3</sub>-Na<sub>2</sub>CO<sub>3</sub>-K<sub>2</sub>CO<sub>3</sub>]<sub>eutectic</sub> from room temperature up to 550°C. The inset represents the absorption edge energy as a function of the spectrum number.

the spectra is observed when increasing the temperature and the spectra observed at 500°C are significantly different from the initial spectra with a 2 eV shift of the shift towards lower energy. This clearly indicates a change in the mean oxidation of Co atoms that is associated to a modification of Co speciation in the sample. A more detailed analysis of this evolution and of the reaction mechanisms will be the subject of a future publication.

##### C. Hydroxides

The case of hydroxides is particularly challenging, as molten hydroxides are highly aggressive. Even glassy carbon and platinum that are inert towards most high temperature aggressive liquids are visually damaged after long experiments with molten hydroxides. We then wanted to test the performance of our set-up, and in particular the cells, in such difficult conditions. The melting temperature of LiOH is 471°C. Similarly to the previous hydrogenosulfate case, the mixture was not heated before the XAS experiment. Pristine LiCoO<sub>2</sub> was mixed with LiOH before being introduced in the cell. The temperature evolution of the spectra is displayed in Fig. 7. In this case, no temperature evolution was observed during the whole run duration, i.e. around 7h. This may be tentatively assigned to an insufficient run duration, as lab-run experiments carried out over one week lead to the appearance of new cobalt species. It may then be worthwhile to run such an experiment again for a longer time although this is not fully adapted to synchrotron-based experiments. It should also be mentioned that after this 7 hours experiment, the boron nitride cell exhibits spots testifying a salt interaction with its wall but with no apparent damage (additional picture is available in the supplementary information file). This experiment

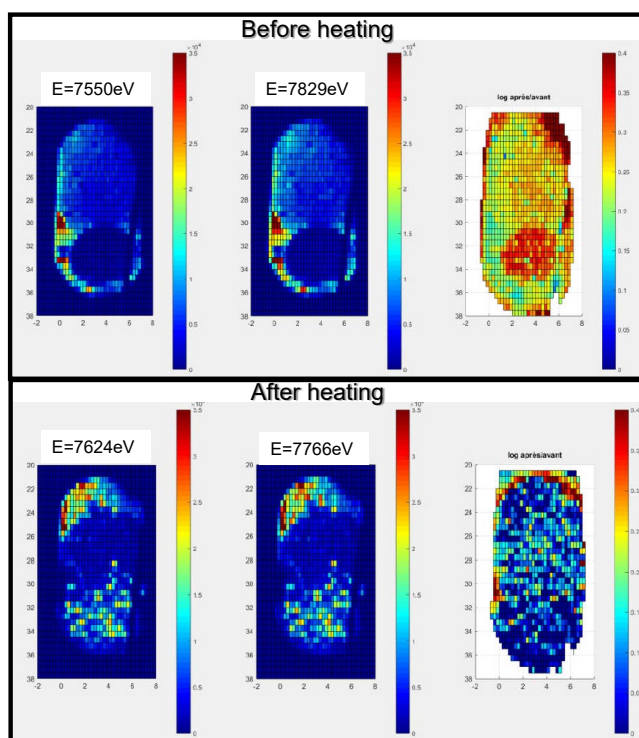


FIG. 5. Cartography of the cell before heating and after heating for intensity before and after Co K edge, and the ratio of the intensity logarithms before and after Co K edge.

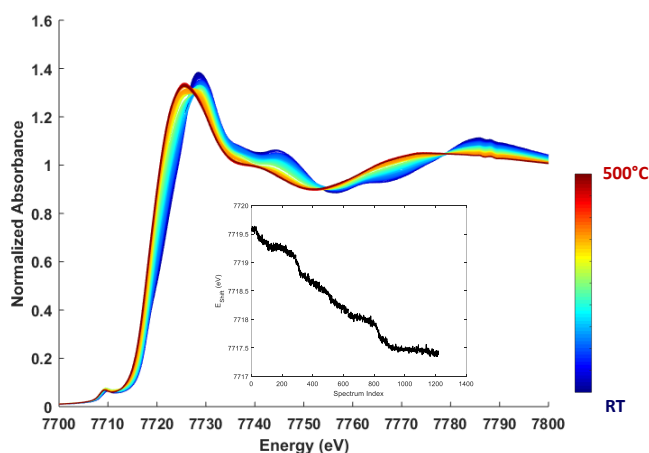


FIG. 6. Co K edge spectra in the case of  $\text{LiCoO}_2$  in  $\text{NaHSO}_4$  from room temperature up to  $500^\circ\text{C}$ . The inset represents the absorption edge energy as a function of the spectrum number.

then demonstrates that our setup can be used for investigating molten hydroxides, provided that the reaction times are not too long.

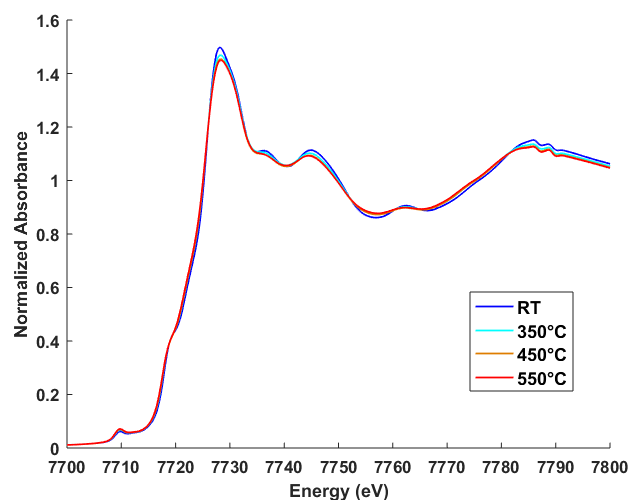


FIG. 7. Co K edge spectra in the case of  $\text{LiCoO}_2$  in  $\text{LiOH}$  at room temperature,  $350^\circ\text{C}$ ,  $450^\circ\text{C}$  and  $550^\circ\text{C}$ .

## V. DISCUSSION

As shown in the three examples presented here, our setup allows measuring X-ray absorption spectra up to  $550^\circ\text{C}$  for molten carbonates and molten hydrogenosulfate over periods of several hours. In the case of highly aggressive media such as molten hydroxides, experiments must be limited to shorter times due to interactions between the molten salt and boron nitride. Compared to other setups reported in the literature and based on more traditional furnaces<sup>31,32,45</sup>, the device presented here bears a definite advantage thanks to the close contact between boron nitride and heating wires that allows fast heating. When combined with the fast recording provided by a Quick-EXAFS beamline such as ROCK, this enables to follow rapid reaction of transition metal compounds in molten salts, as illustrated by the case of  $\text{LiCoO}_2$  in  $\text{NaHSO}_4$  (Fig. 6). It can be estimated that compounds with lifetimes down to a few minutes can be identified with such a combination. The use of a levitation setup using  $\text{CO}_2$  laser heating<sup>38,39,46</sup> allows investigating fast kinetics but is unfortunately not suitable for volatile samples such as molten salts. Furthermore setting and adjusting levitation is rather tricky and extremely difficult to implement for air-sensitive samples.

Furthermore, being able to carry out fast analyses is mandatory when the sample cannot be conditioned within a confining matrix of either boron nitride or other powdered materials. This is for instance the situation of the reduction of  $\text{Co(III)}$  in cobalt oxide with sodium hydrogenosulfate, where the presence of the matrix appears to somehow hinder the reaction, as observed in recent unpublished experiments. In such cases, the liquid nature of molten salt will lead to motions inside the cell, which are worsened by the high-temperature conditions. Such motion will induce dramatic changes in the transmitted intensity over short times. In classical EXAFS beamlines, the recording time is often longer than the macroscopic motion

time of the liquid, which prevents obtaining any reliable spectra. Quick-EXAFS generally overcomes this difficulty as the typical time for collecting one spectrum is around 200ms. It must be emphasized that the issue of liquid motion is even more difficult to solve at medium X-ray energy that imposes the use of very thin samples, in which both gravity and capillary forces lead to liquid motion. Using a reservoir as proposed by Okamoto et al.<sup>31</sup> or by us cannot handle the previously described problem and the use of Quick-EXAFS is then mandatory.

Finally, when studying reaction in transition metals, being able to control the atmosphere around the sample during the reaction is important. This was recognized by Chupas et al.<sup>45</sup> whose design allows adjusting the atmosphere during experiments. Such a feature is not present in our cell, and depending on the sample, the cell can be conditioned either in air or in glove box before being sealed. It must be mentioned that in a few experiments involving carbonates conditioned under air, an over pressure in the sample cavity resulting from the reaction lead to cell explosion. Such event illustrates the tightness of our cell and shows that the atmosphere imposed when sealing will be conserved during the whole course of the experiment.

## VI. CONCLUSION

We presented here the design of a novel device allowing the study by X-ray techniques of molten oxidizing salts at temperatures ranging between room temperature and 650°C. This setup is built around a central boron nitride cell that is in direct contact with heating elements, ensuring an accurate and fast temperature control.

We illustrate the performances of this setup by following by Quick-EXAFS the evolution of Co K edge X-ray absorption spectra of  $\text{LiCoO}_2$  dispersed in three different families of molten salts, i.e. carbonates, hydrogenosulfates, and hydroxides. The proposed design appears perfectly adapted to the case of carbonates and hydrogenosulfates. We show that it can even be employed in the case of highly aggressive hydroxides media, provided that reaction times are kept to less than a few hours.

The combination of fast heating and Quick-EXAFS opens new perspectives for analyzing in detail the reaction mechanisms occurring during pyrochemical processes that represent an attractive recycling route for the recovery of various compounds present in used battery materials. Finally, the setup is rather versatile and could certainly be used for numerous types of samples provided that they do not react with boron nitride at high temperature.

## SUPPLEMENTARY MATERIAL

See supplementary material for additional pictures of the boron nitride cell, of the ceramic chamber and of the cell after long run with molten hydroxide salts.

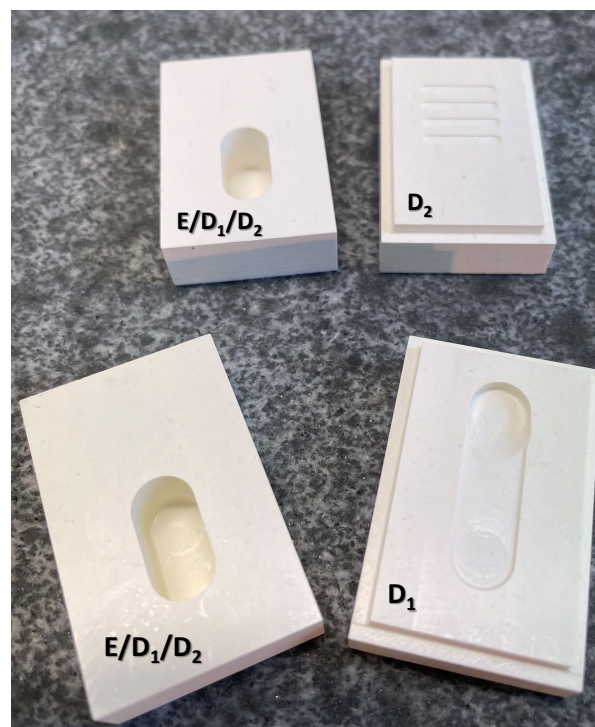


FIG. 8. on the left (top and bottom) external face of the cell part (D<sub>1</sub>, D<sub>2</sub> and E); on the right, internal face of the cell part for D<sub>1</sub> (bottom) and D<sub>2</sub> (top).

### A. Boron Nitride cell

A picture of the internal and external faces of the boron nitride cell is shown in Fig. 8. The internal face of E part is not shown as it is simply a flat boron nitride surface. Each internal face (D<sub>1</sub>, D<sub>2</sub> and E) is carefully flattened in order to ensure the best contact between each parts of the cell. Hence, tightness is achieved. Note that each cell part is machined within one unique boron nitride block.

#### 1. Ceramic chamber

Several views of the ceramic chamber are displayed in Fig. 9.

### B. Boron Nitride cell after experiment with molten hydroxides

As shown in Fig. 10, the aggressive nature of molten hydroxide salts is illustrated by the three horizontal marks present after a run at high temperature. This run consisted in three ramps from room temperature to 200°C, from 200°C to 500°C and from 500 to 550°C separated by three plateaus of 45 minutes at each temperature.



FIG. 9. on the left (top and bottom) external face of the cell part (D<sub>1</sub>, D<sub>2</sub> and E); on the right, internal face of the cell part for D<sub>1</sub> (bottom) and D<sub>2</sub> (top).

## ACKNOWLEDGMENTS

This work was supported by a public grant overseen by the French National Research Agency (ANR) (reference : ANR-18-CE05-0031-01 RELiABLE). We wish to thank I. Senoussaoui, M. Sorriaux, C. Haouari, S. Kang, B. Mercadier, B. Rigaud, F. Lecomte, A. de Souza Braga Neto for their support during the synchrotron experiments. We acknowledge A. G. Porras Gutiérrez for her help during the experiments preparation and T. Krivine and C. Le Bolloch for their investigation of the materials reactivity. The development of the Beamline ROCK was supported by a public grant overseen by the French National Research Agency (ANR) as part of the “Investissements d’Avenir” program (reference : ANR-10-EQPX-45). RS2E was supported by the French National Research Agency (Labex STORE-EX, Grant No. ANR-10-LABX-0076). We are indebted to T. Putaud (LERMA, Sorbonne Université - CNRS, F-75005 Paris, France) for his precious help in Matlab® programming.

## DATA AVAILABILITY STATEMENT

Raw data were generated at the SOLEIL synchrotron large scale facility. Derived data supporting the findings of this study are available from the corresponding author upon reasonable request.



FIG. 10. Picture of the external part of a D<sub>2</sub> type cell containing hydroxide after approximately 6 hours at high temperature.

- <sup>1</sup>A. Hedberg, S. Šipka, and J. Bjerkem, *The circular economy: Going digital* (European Policy Centre, 2020).
- <sup>2</sup>F. K. Zisopoulos, D. F. Schraven, and M. de Jong, “How robust is the circular economy in europe? an ascendancy analysis with eurostat data between 2010 and 2018,” *Resources, Conservation and Recycling* **178**, 106032 (2022).
- <sup>3</sup>X. Liu, M. Tanaka, and Y. Matsui, “Electrical and electronic waste management in china: progress and the barriers to overcome,” *Waste Management & Research* **24**, 92–101 (2006), pMID: 16496875.
- <sup>4</sup>T. Dutta, K.-H. Kim, A. Deep, J. E. Szulejko, K. Vellingiri, S. Kumar, E. E. Kwon, and S.-T. Yun, “Recovery of nanomaterials from battery and electronic wastes: A new paradigm of environmental waste management,” *Renewable and Sustainable Energy Reviews* **82**, 3694–3704 (2018).
- <sup>5</sup>B. Scrosati, K. M. Abraham, W. V. Schalkwijk, and J. Hassoun, *Lithium Batteries: Advanced Technologies and Applications* (John Wiley Sons, 2013).
- <sup>6</sup>M. Al Sakka, A. Benmayza, W. Bernhart, Y. Borthomieu, A. Brecher, A. Burke, A. Dallaire, A. Dell’Era, J. Dubé, J. B. Dunn, U. Eberle, W. Fang, D. D. Friel, L. L. Gaines, K. G. Gallagher, K. Galoustov, H. Gualous, A. Guerfi, H. Horie, N. S. Hudak, H. Iba, J. Jeevarajan, C. M. Julien, K. Maher, R. Matthé, A. Mauger, F. Mizuno, P. A. Nelson, Y. Nishi, N. Omar, F. Orecchini, J. Prakash, P. Ramadass, M. Ramanathan, L. Rohr, A. Samba, A. Santiangeli, P. Van den Bossche, J. Van Mierlo, M. Vetter, A. Vezzini, J. Warner, M. Weil, C. Yada, J. ichi Yamaki, R. Yazami, A. Yoshino, K. Zaghib, Z. J. Zhang, and S. Ziemann, *Lithium-Ion Batteries*, edited by G. Pistoia (Elsevier, Amsterdam, 2014).
- <sup>7</sup>W. Lv, Z. Wang, H. Cao, Y. Sun, Y. Zhang, and Z. Sun, “A critical review and analysis on the recycling of spent lithium-ion batteries,” *ACS Sustainable Chemistry & Engineering* **6**, 1504–1521 (2018).
- <sup>8</sup>J. Ordoñez, E. Gago, and A. Girard, “Processes and technologies for the recycling and recovery of spent lithium-ion batteries,” *Renewable and Sustainable Energy Reviews* **60**, 195–205 (2016).
- <sup>9</sup>J. Xu, H. Thomas, R. W. Francis, K. R. Lum, J. Wang, and B. Liang, “A review of processes and technologies for the recycling of lithium-ion secondary batteries,” *Journal of Power Sources* **177**, 512–527 (2008).
- <sup>10</sup>P. Meshram, A. Mishra, Abhilash, and R. Sahu, “Environmental impact of spent lithium ion batteries and green recycling perspectives by organic acids – a review,” *Chemosphere* **242**, 125291 (2020).
- <sup>11</sup>B. Zhang, H. Xie, B. Lu, X. Chen, P. Xing, J. Qu, Q. Song, and H. Yin, “A green electrochemical process to recover co and li from spent licoo<sub>2</sub>-based batteries in molten salts,” *ACS Sustainable Chemistry & Engineering* **7**,

- 13391–13399 (2019).
- <sup>12</sup>T. Amietszajew, S. Sridhar, and R. Bhagat, “Metal recovery by electrodeposition from a molten salt two-phase cell system,” *Journal of The Electrochemical Society* **163**, D515–D521 (2016).
  - <sup>13</sup>R. C. Ortiz, T. Amietszajew, and R. Bhagat, “Recovery of nickel and cobalt by electrowinning from spent lithium-ion batteries using molten salt electrolytes,” *ECS Meeting Abstracts* **MA2020-02**, 1536–1536 (2020).
  - <sup>14</sup>M. Galopin and J. Daniel, “Molten salts in metal treating: Present uses and future trends,” *Electrodeposition and Surface Treatment* **3**, 1–31 (1975).
  - <sup>15</sup>F. L. Henri Groult, ed., *Molten Salts Chemistry: From Lab to Application* (Elsevier, Amsterdam, 2013).
  - <sup>16</sup>K. I. Popov, S. S. Djokić, and B. N. Grgur, *Fundamental Aspects of Electrometallurgy* (Springer, Boston, 2002).
  - <sup>17</sup>T. Inoue, “Actinide recycling by pyro-process with metal fuel fbr for future nuclear fuel cycle system,” *Progress in Nuclear Energy* **40**, 547–554 (2002).
  - <sup>18</sup>P. Taxil, L. Massot, C. Nourry, M. Gibilaro, P. Chamelot, and L. Cassayre, “Lanthanides extraction processes in molten fluoride media: Application to nuclear spent fuel reprocessing,” *Journal of Fluorine Chemistry* **130**, 94–101 (2009), fluorine Nuclear Energy.
  - <sup>19</sup>S. Bourg, “The chemical basis for separating recycling materials by pyro-processes,” in *Encyclopedia of Nuclear Energy*, edited by E. Greenspan (Elsevier, Oxford, 2021) pp. 465–481.
  - <sup>20</sup>Z. Yao, J. Li, and X. Zhao, “Molten salt oxidation: A versatile and promising technology for the destruction of organic-containing wastes,” *Chemosphere* **84**, 1167–1174 (2011).
  - <sup>21</sup>P. C. Hsu, K. G. Foster, T. D. Ford, P. Wallman, B. E. Watkins, C. O. Pruneda, and M. G. Adamson, “Treatment of solid wastes with molten salt oxidation,” *Waste Management* **20**, 363–368 (2000).
  - <sup>22</sup>A. Fedorov, Y. Chekryshkin, and A. Gorbunov, “Studies of recycling of poly(vinyl chloride) in molten na, ca ll no<sub>3</sub>, oh systems,” *International Scholarly Research Notices*, 768134 (2012).
  - <sup>23</sup>H.-C. Yang, Y.-J. Cho, H.-C. Eun, and E.-H. Kim, “Destruction of chlorobenzene and carbon tetrachloride in a two-stage molten salt oxidation reactor system,” *Chemosphere* **73**, S311–S315 (2008), halogenated Persistent Organic Pollutants Dioxin 2005.
  - <sup>24</sup>Z. Yao, X. Zhao, and J. Li, “Study on 1,2,3-trichlorobenzene destruction in a binary (na,k)2co<sub>3</sub> molten salt oxidation system,” *Environmental Progress & Sustainable Energy* **33**, 65–69 (2014), <https://aiche.onlinelibrary.wiley.com/doi/pdf/10.1002/ep.11751>.
  - <sup>25</sup>S. Dai, Y. Zheng, Y. Zhao, Y. Chen, and D. Niu, “Molten hydroxide for detoxification of chlorine-containing waste: Unraveling chlorine retention efficiency and chlorine salt enrichment,” *Journal of Environmental Sciences* **82**, 192–202 (2019).
  - <sup>26</sup>G. E. Bertolini and J. Fontaine, “Value recovery from plastics waste by pyrolysis in molten salts,” *Conservation Recycling* **10**, 331–343 (1987), recycling in Japan: a Status Report.
  - <sup>27</sup>O. Takeda, D. Aoki, Y. Yokka, T. Yamamura, and Y. Sato, “Decomposition of mono-, di- and tri-chlorobenzene by using basic molten salts,” *ISIJ International* **52**, 1705–1711 (2012).
  - <sup>28</sup>D. D. Williams, J. A. Grand, and R. R. Miller, “The reactions of molten sodium hydroxide with various metals1,” *Journal of the American Chemical Society* **78**, 5150–5155 (1956), <https://doi.org/10.1021/ja01601a004>.
  - <sup>29</sup>M. Anisur, A. Aphale, M. Reiser, P. K. Dubey, S. J. Heo, J. Hong, K. Patil, H. Xu, C.-Y. Yuh, and P. Singh, “Stability of ceramic matrix materials in molten hydroxide under oxidizing and reducing conditions,” *International Journal of Hydrogen Energy* **46**, 14898–14912 (2021), international Workshop of Molten Carbonates Related Topics 2019 (IWMC2019).
  - <sup>30</sup>A. D. Cicco, “Local structure in binary liquids probed by EXAFS,” *Journal of Physics: Condensed Matter* **8**, 9341–9345 (1996).
  - <sup>31</sup>Y. Okamoto, M. Akabori, H. Motohashi, H. Shiwaku, and T. Ogawa, “X-ray absorption study of molten yttrium trihalides,” *Journal of Synchrotron Radiation* **8**, 1191–1199 (2001).
  - <sup>32</sup>A.-L. Rollet, C. Bessada, Y. Auger, P. Melin, M. Gailhanou, and D. Thiaudière, “A new cell for high temperature exafs measurements in molten rare earth fluorides,” *Nuclear Instruments and Methods in Physics Research Section B: Beam Interactions with Materials and Atoms* **226**, 447–452 (2004).
  - <sup>33</sup>H. Matsuura, A. Nezu, H. Akatsuka, S. Watanabe, A. Kajinami, Y. Iwate, and N. Umesaki, “In-situ observation technique of electrodeposition reaction by x-ray from synchrotron source,” *Progress in Nuclear Energy* **53**, 930–934 (2011), the Third International Symposium on Innovative Nuclear Energy Systems, INES-3- Innovative Nuclear Technologies for Low-Carbon Society.
  - <sup>34</sup>S. Watanabe, A. K. Adya, L. Rycerz, A. C. Barnes, M. Gaune-Escard, Y. Okamoto, H. Akatsuka, and H. Matsuura, “Xafs study of europium chloride at high temperatures,” *Progress in Nuclear Energy* **47**, 632–638 (2005).
  - <sup>35</sup>Y.-C. Liu, Y.-L. Liu, L. Wang, Y.-K. Zhong, M. Li, W. Han, Y. Zhao, T. Zhou, Q. Zou, X. Zeng, and W.-Q. Shi, “Uranium chemical species in licl-kcl eutectic under different conditions for the dissolution of u3o8,” *Journal of Nuclear Materials* **542**, 152475 (2020).
  - <sup>36</sup>C. Bessada, D. Zanghi, O. Pauvert, L. Maksoud, A. Gil-Martin, V. Saroukanian, P. Melin, S. Brassamin, A. Nezu, and H. Matsuura, “High temperature exafs experiments in molten actinide fluorides: The challenge of a triple containment cell for radioactive and aggressive liquids,” *Journal of Nuclear Materials* **494**, 192–199 (2017).
  - <sup>37</sup>A. L. Smith, M. N. Verleg, J. Vlieland, D. de Haas, J. A. Ocadiz-Flores, P. Martin, J. Rothe, K. Dardenne, M. Salanne, A. E. Gheribi, E. Capelli, L. van Eijck, and R. J. M. Konings, “*In situ* high-temperature EXAFS measurements on radioactive and air-sensitive molten salt materials,” *Journal of Synchrotron Radiation* **26**, 124–136 (2019).
  - <sup>38</sup>C. Landron, X. Launay, J. Rifflet, P. Echegut, Y. Auger, D. Ruffier, J. Coutures, M. Lemonier, M. Gailhanou, M. Bessiere, D. Bazin, and H. Dexpert, “Development of a levitation cell for synchrotron radiation experiments at very high temperature,” *Nuclear Instruments and Methods in Physics Research Section B: Beam Interactions with Materials and Atoms* **124**, 627–632 (1997).
  - <sup>39</sup>C. Landron, L. Hennet, D. Thiaudière, D. Price, and G. Greaves, “Structure of liquid oxides at very high temperatures,” *Nuclear Instruments and Methods in Physics Research Section B: Beam Interactions with Materials and Atoms* **199**, 481–488 (2003).
  - <sup>40</sup>A. C. D’Orazio, T. Marshall, T. Sultana, J. K. Gerardi, C. U. Segre, J. P. Carlo, and B. C. Eigenbrodt, “High temperature x-ray absorption spectroscopy of the local electronic structure and oxide vacancy formation in the sr2fe1.5mo0.5o6 solid oxide fuel cell anode catalyst,” *ACS Applied Energy Materials* **2**, 3061–3070 (2019).
  - <sup>41</sup>V. Briois, C. L. Fontaine, S. Belin, L. Barthe, T. Moreno, V. Pinty, A. Carcy, R. Girardot, and E. Fonda, “ROCK: the new quick-EXAFS beamline at SOLEIL,” *Journal of Physics: Conference Series* **712**, 012149 (2016).
  - <sup>42</sup>Y. Okamoto, M. Akabori, H. Motohashi, A. Itoh, and T. Ogawa, “High-temperature xafs measurement of molten salt systems,” *Nuclear Instruments and Methods in Physics Research Section A: Accelerators, Spectrometers, Detectors and Associated Equipment* **487**, 605–611 (2002).
  - <sup>43</sup>C. Lesage, E. Devers, C. Legens, G. Fernandes, O. Roudenko, and V. Briois, “High pressure cell for edge jumping x-ray absorption spectroscopy: Applications to industrial liquid sulfidation of hydrotreatment catalysts,” *Catalysis Today* **336**, 63–73 (2019), selected papers from the 6th International Congress on Operando Spectroscopy.
  - <sup>44</sup>A. Rollet, A. Rakhmatullin, and C. Bessada, “Local structure analogy of lanthanide fluoride molten salts,” *International Journal of Thermophysics* **26**, 1115–1125 (2005).
  - <sup>45</sup>P. J. Chupas, K. W. Chapman, C. Kurtz, J. C. Hanson, P. L. Lee, and C. P. Grey, “A versatile sample-environment cell for non-ambient X-ray scattering experiments,” *Journal of Applied Crystallography* **41**, 822–824 (2008).
  - <sup>46</sup>M. Capron, P. Florian, F. Fayon, D. Trumeau, L. Hennet, M. Gailhanou, D. Thiaudière, C. Landron, A. Douy, and D. Massiot, “Local structure and dynamics of high temperature sro–al2o3 liquids studied by 27al nmr and sr k-edge xas spectroscopy,” *Journal of Non-Crystalline Solids* **293-295**, 496–501 (2001), 8th Int. Conf. on Non-Crystalline Materials.